

AN OPTICAL TRACKING APPROACH TO COMPUTER-ASSISTED SURGICAL NAVIGATION VIA STEREOSCOPIC VISION

Darin Tsui, Capalina Melentyev, Ananya Rajan, Rohan Kumar, and Frank E. Talke*

Center for Memory and Recording Research (CMRR), University of California San Diego, San Diego, CA

ABSTRACT

Computer-assisted navigation has become a popular solution in surgical procedures where a high amount of precision is required. Current state-of-the-art methods of surgical navigation involve tracking reflective 3D marker spheres using IR stereoscopic cameras. However, the cost of implementing such systems may not be affordable for smaller healthcare systems. In this paper, we propose that fully optical navigation has the potential to be a viable alternative to state-of-the-art reflective marker navigation. We use fiducial ArUco markers to facilitate the tracking of real-time position. Using two inexpensive cameras, we design and calibrate a stereoscopic camera to record the 3D position of an ArUco marker moving through space along a positioning platform. Additionally, we explore the possibility of using different color spaces and physical marker colors to improve the detection percentage and accuracy of markers. We identified that black-and-white ArUco markers using the Hue, Saturation, and Lightness (HSL) color space gave a positional mean error of 5.38 mm. Using the Red, Green, and Blue (RGB) color space gave the highest detection percentage for the same ArUco markers. In the future, the mean error can be reduced by increasing camera quality and by using a multi-stereoscopic camera setup.

Keywords: surgical navigation, computer-assisted surgery, stereoscopic vision, fiducial ArUco markers

1. INTRODUCTION

In recent years, surgical navigation systems have seen usage in many medical fields, including neurosurgery, orthopedic surgery, and maxillofacial surgery [1]. One of the main reasons for the implementation of such navigation systems is their ability to provide real-time guidance to surgeons during minimally invasive procedures [2]. As such, current state-of-the-art navigation systems are able to provide surgeons with high positional precision, thus improving the success of surgery [3].

Existing approaches to surgical navigation revolve around the usage of infrared (IR) stereoscopic cameras where retro-reflective

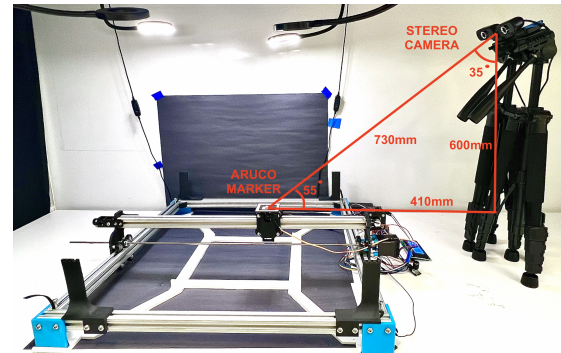


FIGURE 1: EXPERIMENTAL SETUP OF THE STEREOSCOPIC CAMERA RELATIVE TO THE POSITIONING PLATFORM

markers are made visible to near-infrared stereoscopic cameras [3, 4]. Although these systems are reliable, they are expensive. On the other hand, fully optical, or videometric tracking, uses a calibrated camera to track patterned markers. This technology is more accessible to healthcare institutions due to its low cost [5]. In this paper, we propose that the use of stereoscopic, videometric tracking with fiducial markers has the potential to be a low-cost alternative in surgical navigation.

2. METHODS

2.1 Stereoscopic Camera Setup

To establish that optical marker tracking is a promising alternative to traditional surgical navigation systems, we developed an inexpensive tracking system, as seen in Fig. 1, using off-the-shelf parts. For 3D positional tracking, we calibrated a stereoscopic camera system using two web cameras (HZQDLN HD). At the time of this publication, these cameras retail for \$30. This makes the total cost of the stereoscopic system significantly cheaper compared to other state-of-the-art navigation systems. Figure 2 displays our stereo camera setup. The distance between the two cameras is 73 mm.

We calibrated our stereoscopic camera system using an 8 by 11 calibration checkerboard, in accordance with calibration

*Corresponding author: ftalke@ucsd.edu



FIGURE 2: STEREOSCOPIC CAMERA SETUP

checkerboard documentation [6]. OpenCV was used to obtain intrinsic camera parameters, which include the focal length and optical centers.

2.2 Marker Tracking Implementation

We implemented the ArUco marker package through OpenCV to facilitate positional tracking. ArUco markers are part of a square-based fiducial marker system that specializes in camera pose estimation [7]. As the ArUco marker moves in space, the stereoscopic camera tracks the center position of the marker. Given the centers of the ArUco marker as seen by the two cameras, we can compute the disparity between the markers. The disparity, d , is defined as the difference in horizontal position between the left (x_l) and right (x_r) cameras.

With the focal length f and baseline distance b of the camera and the disparity d , we are able to compute the 3D position of the marker using equations (2-4). Here, y_l is the vertical position of the marker in the left camera.

$$d = x_l - x_r \quad (1)$$

$$z = \frac{fb}{d} \quad (2)$$

$$x = \frac{x_l z}{f} \quad (3)$$

$$y = \frac{y_l z}{f} \quad (4)$$

2.3 Experimental Setup

To test the accuracy of the stereo camera and positioning algorithm on moving markers, we developed a positioning platform to move the marker in the X and Y directions as seen in Fig. 3. We also label the position of the marker in 3D space (x, y, z). We use two motors to move the marker in a square pattern. In our experiments, the moving marker was shuttled around following the pattern shown in Fig. 4.

During experiments, we placed our stereo camera on a tripod at a distance of 410 mm away from the center of the marker's starting point. The stereo camera captured the moving marker at a 35-degree angle at a height of 600 mm. Light of intensity 37 lux was provided by a ring LED. Figure 1 displays the complete setup of the experiment.

2.4 Marker Tracking Experiments

To integrate optical tracking into surgical navigation, it is important to explore the parameters that would best optimize the reliability and accuracy of navigation. For this paper, we explore two parameters: color space conversion and the marker's physical color.

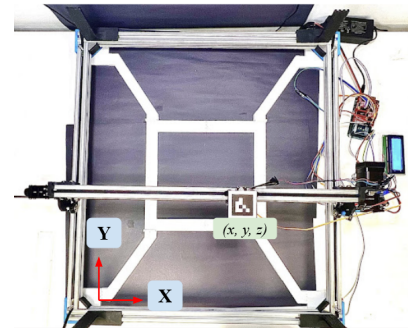


FIGURE 3: POSITIONING PLATFORM SETUP. THE MOVING MARKER IS ABLE TO MOVE IN THE X AND Y DIRECTIONS

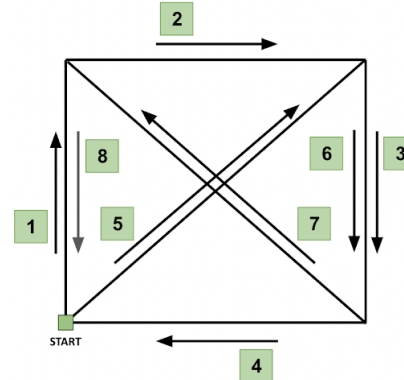


FIGURE 4: MARKER MOVEMENT PATTERN, DISPLAYING THE ORDER OF MOVEMENT

In all marker tracking experiments, the ArUco marker moved at a speed of 20 mm/sec. The markers used for these experiments had a width of 40 mm and a pixel density of 4x4. The pixel density is defined as the number of bits, or inner squares, of the ArUco marker. Three trials were performed for all experiments.

2.5 Color Space Conversions and Marker Color

Upon capturing live video of the marker moving on the positioning platform, we converted the video frames to different color spaces. Marker tracking tests were performed in Red, Green, and Blue (RGB), Hue, Saturation, and Lightness (HSL), and Hue, Saturation, and Value (HSV) color spaces. These color spaces were chosen as they are the most commonly used in image processing. When converting from RGB to HSL or HSV, thresholding was performed on the output. In HSL, the lower threshold for Lightness (L) was chosen to be 50%. In HSV, the lower threshold for Value (V) was set to 55%. Hue and Saturation remained the same. Additionally, we also varied the color of the ArUco marker to see its impact in the different color spaces. We tested white, pink, yellow, and orange-colored markers, as seen in Fig. 5.

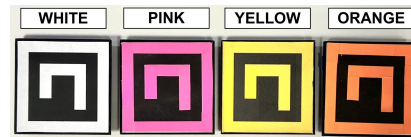


FIGURE 5: COLORED ARUCO MARKERS THAT WERE TESTED

TABLE 1: DETECTION PERCENTAGE (%) OF FOUR COLORED MARKERS IN RGB, HSL AND HSV COLOR SPACES

Color Space	Color			
	White	Pink	Yellow	Orange
RGB	99.7	98.1	97.1	99.5
HSL	99.5	81.3	89.7	87.0
HSV	97.5	73.5	78.4	80.6

TABLE 2: MARKER TRACKING AVERAGE ERROR (MM) OF FOUR COLORED MARKERS IN RGB, HSL, AND HSV

Color Space	Color			
	White	Pink	Yellow	Orange
RGB	5.48	5.62	12.35	5.39
HSL	5.38	6.80	5.96	6.26
HSV	5.61	6.98	6.17	5.88

2.6 3D Mapping Verification of Marker Position

Upon obtaining the 3D position of the marker from the stereo camera's perspective, we evaluated the positional accuracy of the camera by projecting the marker's position from camera coordinates (x, y, z) to real-world coordinates (X, Y). To do this, we transformed the 3D coordinates of the markers onto the X-Y plane using the corners of the marker movement square. A homography matrix was computed to convert the marker coordinates of the camera to real-life distances. The coordinates used to perform homography were taken from the corners of the marker movement square. Following the conversion to real-life distances, the error was calculated by comparing the real-life distance the marker moves to the distance the marker moves in world coordinates.

3. RESULTS AND DISCUSSION

3.1 Results

To determine the reliability of the optical tracking system, we report our results in terms of detection percentage. To calculate this, we compared the total amount of frames captured to the amount of times the marker was detected as it moved.

Table 1 reports the detection percentage observed when tracking the differently colored moving markers in the three color spaces. Table 2 reports the mean error across all three trials when tracking differently colored moving markers in the three color spaces. It is evident that the RGB colorspace performs best for all colors. Additionally, when comparing the colors, it can be seen that the white marker consistently had the best accuracy. From the results shown in Table 2, we can see that the white marker in the HSL colorspace performs the best.

3.2 Discussion

Based on the results in Section 3.1, the development of a fully optical surgical navigation system is promising. While the mean error of the present system is higher than what is needed for clinical use, the fact that the stereoscopic system was created using inexpensive, off-the-shelf parts demonstrates the potential of such a system with further optimization.

To reduce the error of the system, several improvements could be implemented. For one, recreating the stereoscopic system with higher quality cameras would improve the accuracy of the system, as well as increase marker detection percentage regardless of the color space and marker color used. Additionally, designing a multi-stereoscopic camera system would likely improve detection and accuracy of the system. From here, one could find the marker position by taking a weighted average of the two camera positions depending on which camera is closer to the marker.

4. CONCLUSION

In this study, we have designed and calibrated a stereoscopic camera to record the 3D position of a moving ArUco marker. We explored the accuracy and detection percentage of the ArUco marker by varying color spaces and the marker's physical color. A positioning platform was used to evaluate the accuracy of the stereoscopic system. Using black-and-white ArUco markers in the HSL color space, we obtained a mean error of 5.38 mm.

ACKNOWLEDGMENTS

Research towards this project was supported by the UCSD General Campus Research Senate Grant 2019201.

REFERENCES

- [1] Zhang, Mengshi, et al., 2019. "Multiple Instruments Motion Trajectory Tracking in Optical Surgical Navigation." *Optics Express* 27 (11): 15827. <https://doi.org/10.1364/oe.27.015827>.
- [2] Contreras López, et al., 2019. "Intraoperative Clinical Application of Augmented Reality in Neurosurgery: A Systematic Review." *Clinical Neurology and Neurosurgery* 177 (February):6–11.<https://doi.org/10.1016/j.clineuro.2018.11.018>.
- [3] Mezger, Uli, Claudia Jendrewski, and Michael Bartels. 2013. "Navigation in Surgery." *Langenbeck's Archives of Surgery* 398 (4): 501–14. <https://doi.org/10.1007/s00423-013-1059-4>.
- [4] Wu, Han, et al., 2019. "An Accurate Recognition of Infrared Retro-Reflective Markers in Surgical Navigation." *Journal of Medical Systems* 43 (6). <https://doi.org/10.1007/s10916-019-1257-x>.
- [5] Sorriento, Angela, et al., 2020. "Optical and Electromagnetic Tracking Systems for Biomedical Applications: A Critical Review on Potentialities and Limitations." *IEEE Reviews in Biomedical Engineering* 13: 212–32. <https://doi.org/10.1109/rbme.2019.2939091>.
- [6] Zhengyou Zhang. 2004. "Camera Calibration with One-Dimensional Objects." *IEEE Transactions on Pattern Analysis and Machine Intelligence* 26 (7): 892–99. <https://doi.org/10.1109/tpami.2004.21>.
- [7] Garrido-Jurado, et al., 2014. "Automatic Generation and Detection of Highly Reliable Fiducial Markers under Occlusion." *Pattern Recognition* 47 (6): 2280–92. <https://doi.org/10.1016/j.patcog.2014.01.005>.